The Island Arc (2004) **13,** 403–415

Research Article

Thrust geometries in unconsolidated Quaternary sediments and evolution of the Eupchon Fault, southeast Korea

YOUNG-SEOG KIM,[1,*] JOON YOUNG PARK,[1] JEONG HWAN KIM,[1] HYEON CHO SHIN[2] AND DAVID J. SANDERSON[3]

[1]*School of Earth and Environmental Sciences, Seoul National University, Seoul 151-747, Korea (email: ysk7909@snu.ac.kr),* [2]*Korea Power Engineering Company (KOPEC), Yongin 449-912, Korea and* [3]*Department of Earth Science and Engineering, Imperial College, London SW7 2AZ, UK*

Abstract The Korean peninsula is widely regarded as being located at the relatively stable eastern margin of the Asian continent. However, more than 10 Quaternary faults have recently been discovered in and reported from the southeastern part of the Korean Peninsula. One of these, the Eupchon Fault, was discovered during the construction of a primary school, and it is located close to a nuclear power plant. To understand the nature and characteristics of the Quaternary Eupchon Fault, we carried out two trench surveys near the discovery site. The fault system includes one main reverse fault (N20°E/40°SE) with approximately 4 m displacement, and a series of branch faults, cutting unconsolidated Quaternary sediments. Structures in the fault system include synthetic and antithetic faults, hanging-wall anticlines, drag folds, back thrusts, pop-up structures, flat-ramp geometries and duplexes, which are very similar to those seen in thrust systems in consolidated rocks. In the upper part of the fault system, several tip damage zones are observed, indicating that the fault system propagates upward and terminates in the upper part of the section. Pebbles along the main fault plane show a preferred orientation of long axes, indicating the fault trace. The unconformity surface between the Quaternary deposits and the underlying Tertiary andesites or Cretaceous sedimentary rocks is displaced by this fault with a reverse movement sense. The stratigraphic relationship shows normal slip sense at the lower part of the section, indicating that the fault had a normal slip movement and was reversely reactivated during the Quaternary. The inferred length of the Quaternary thrust fault, based on the relationship between fault length and displacement, is 200–2000 m. The current maximum horizontal compressive stress direction in this area is generally east-northeast–west-southwest, which would be expected to produce oblique slip on the Eupchon Fault, with reverse and right-lateral strike-slip components.

Key words: Eupchon, geometry, Quaternary, reactivation, southeast Korea, thrust fault, unconsolidated sediment.

INTRODUCTION

The Korean peninsula is considered to be a relatively stable margin of the Asian continent, but faults related to Quaternary tectonic movements have been reported recently from the southeastern part of the peninsula (KIGAM 1998; Ryoo *et al.* 2000; Chang 2001; Kyung & Chang 2001; Choi *et al.* 2002b; Ryoo *et al.* 2002; Ree *et al.* 2003). The most recent activated faulting was approximately 2000 years ago (Kyung & Chang 2001). Most of the known Quaternary faults are located around the Yangsan and Ulsan faults in the Gyeongsang Basin of the southeastern part of the peninsula (Fig. 1; e.g. Choi *et al.* 2002b). Some of the faults affect Quaternary alluvial fans or colluvial

*Correspondence.

Received 15 October 2003; accepted for publication 13 February 2004.

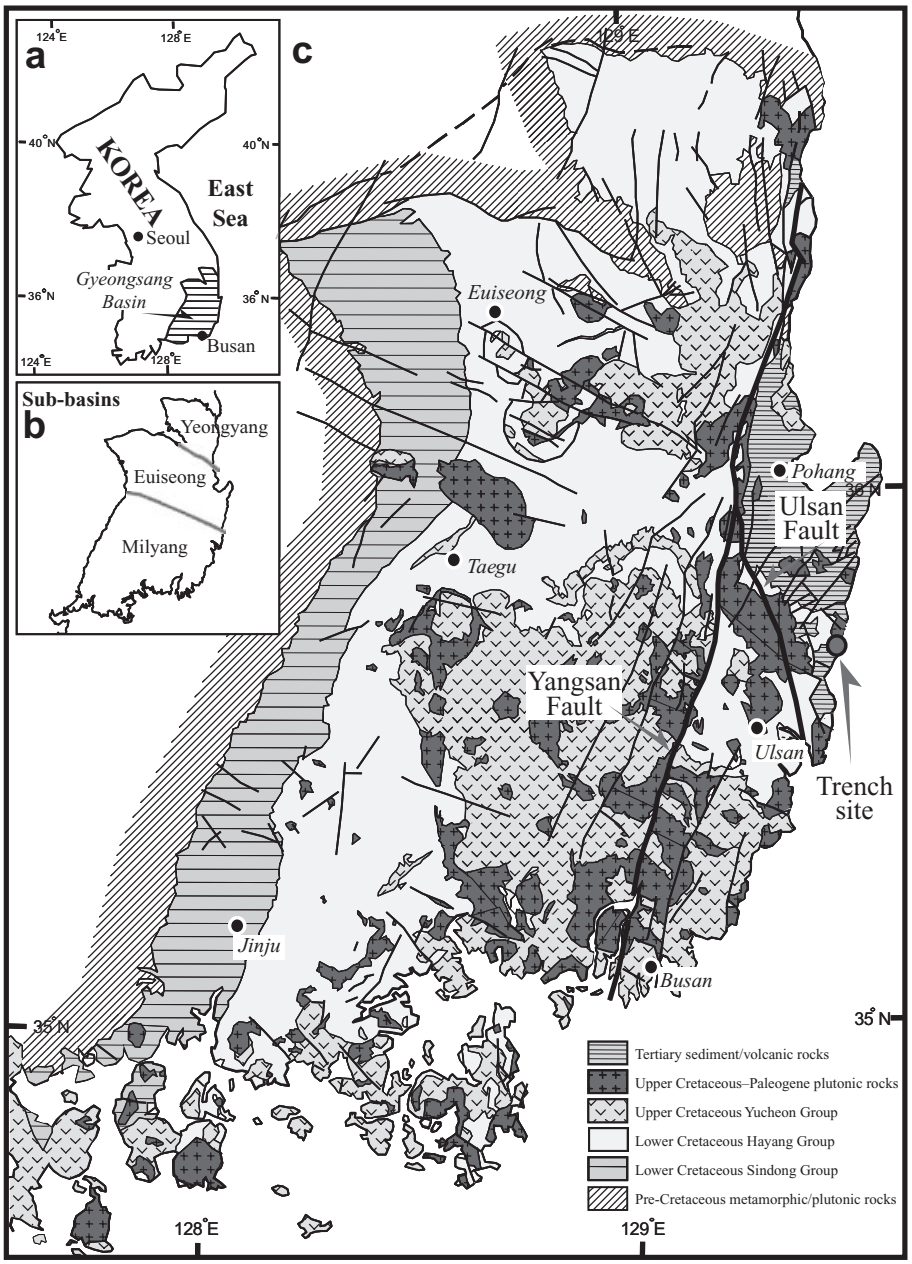

Fig. 1 Locality map of the study area (a,b) and geological map of the southeastern part of the Korean Peninsula (c; modified from Lee 2000). The Gyeongsang Basin is divided into three subbasins (b). The Tertiary and Quaternary sediments are dominantly developed to the east of the north-northeast–south-southwest-trending Yangsan Fault and the north-northwest–south-southeast-trending Ulsan Fault.

deposits (e.g. Wangsan, Malbang and Ipsil faults), and others affect Quaternary marine terrace deposits (e.g. Eupchon and Suryum faults). Although some of these faults have been investigated in detail, particularly the Suryum and Eupchon faults (KIGAM 1998; KOPEC 2002; Choi *et al.* 2003; Ree *et al.* 2003), there has been little detailed structural analysis of these faults.

The Quaternary faults in the southeastern part of the Korean Peninsula are particularly interesting because of their proximity to the Weolsung Nuclear Power Plant (Fig. 2). The Eupchon Fault is located only 1.8 km away from the plant. The nature, scale and activity of the fault are the subject of this paper, including a discussion of the probable fault length. The characteristics of the fault and the stress conditions are very important for reactivation of the fault. However, the age, number of slip events and length of the fault are still controversial.

To clarify the characteristics of the Quaternary Eupchon Fault, we carried out two trench surveys near the first observed site of the fault (Figs 2,3). These were constructed during winter for safety from landslides on steep slopes. Deformation patterns in unconsolidated sediments have not been well documented. This study shows that the structure of reverse fault systems in unconsolidated

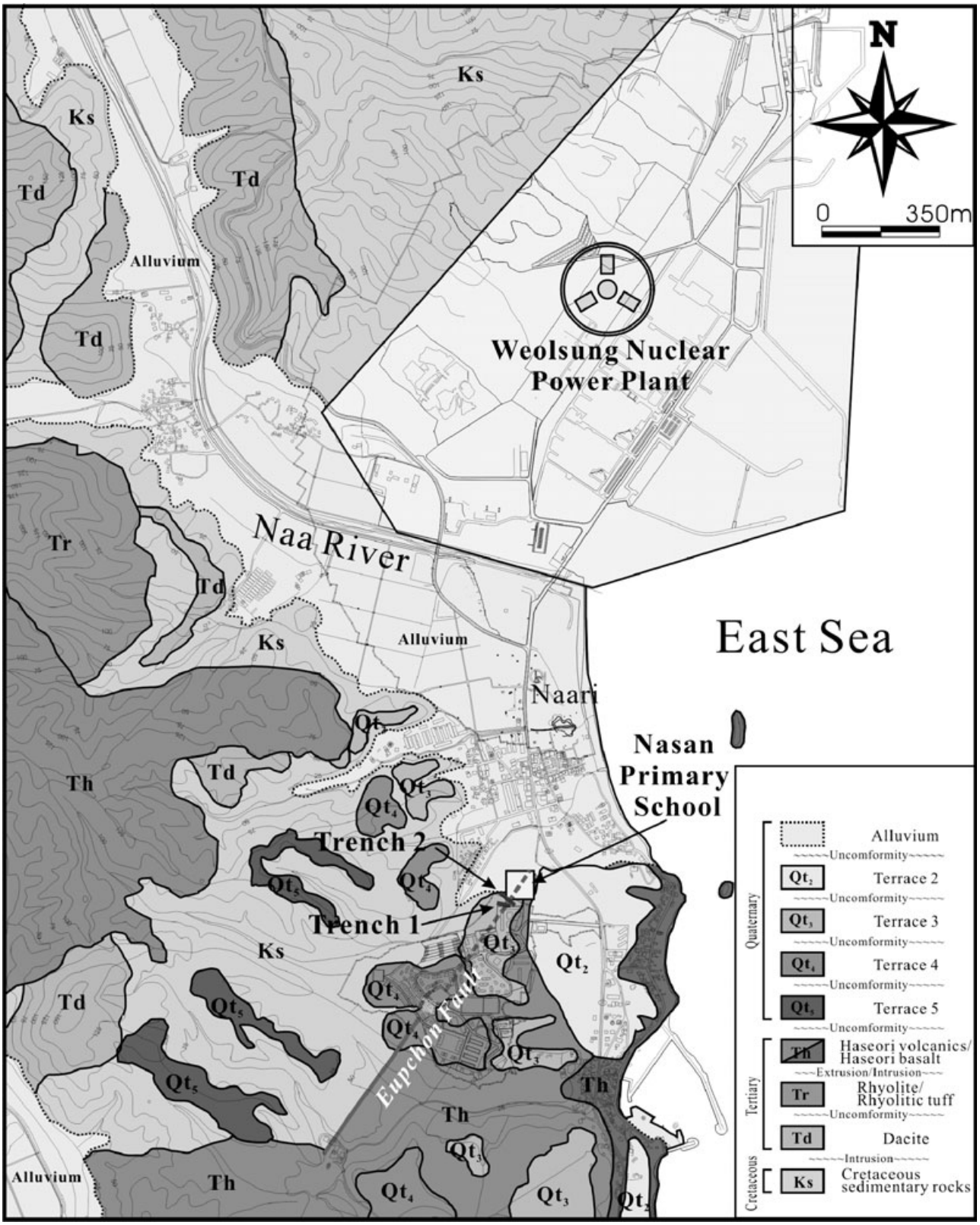

Fig. 2 Geological map of the study area and trench location. The area consists of Cretaceous sedimentary rocks, and various later igneous and sedimentary rocks. Marine terrace sediments are developed along the coastline with various levels (modified from KOPEC 2002). The dashed reverse fault indicates the inferred trace of the Eupchon Fault.

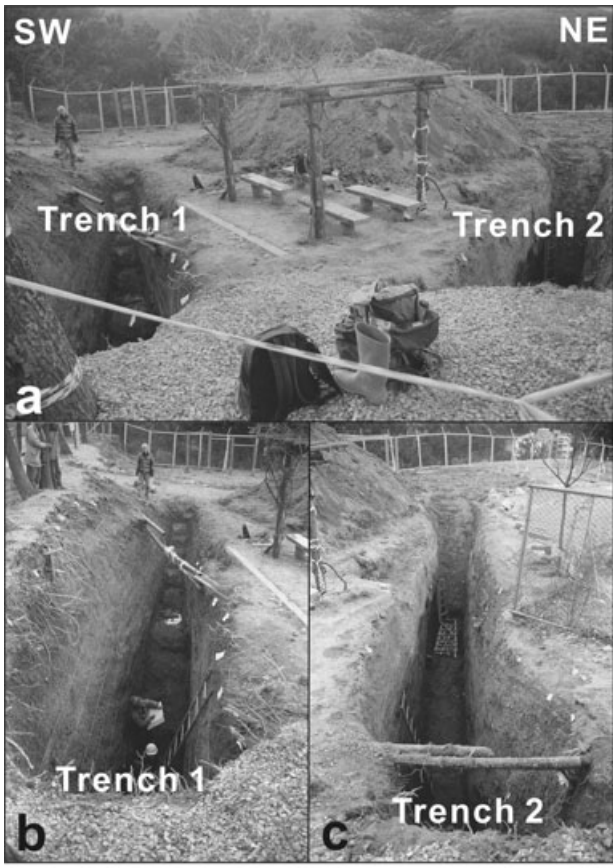

Fig. 3 The two trenches. (a) Photograph looking to the northwest. The orientations of Trench 1 (b) and Trench 2 (c) are 170° and 150°, respectively, and they are at a high angle to the strike of the fault. The widths of Trench 1 and Trench 2 are 1.5 and 1.3 m, and the maximum depths are 5.5 and 2.8 m, respectively.

sediments is very similar to those of thrust systems in consolidated rocks (e.g. Dahlstrom 1970; Boyer & Elliott 1982; Butler 1982).

TECTONIC AND GEOLOGICAL SETTINGS

The basement rocks in the study area are Cretaceous sediments forming part of the Gyeongsang Basin in southeast Korea (Fig. 1). The Cretaceous rocks in this area comprise interbedded sandstone and shale, and they have a fairly consistent strike (N10°–20°E) and dip (30°–60°NW), except where locally disturbed by faults. They are intruded by Cretaceous and Tertiary igneous rocks, predominantly granites.

It is suggested that the intraplate deformation of microplates, caused by the retreat of the Amurian Plate from the Japan Trench, initiated the back-arc rifting and spreading of the East Sea (or Japan Sea) in the late Oligocene to early Miocene (Kimura & Tamaki 1986; Tamaki 1988; Kaneoka *et al.* 1992; Yoon & Chough 1995). The development of the Tertiary basins along the eastern margin of the Gyeongsang Basin is associated with the extension of the East Sea (or Japan Sea). In the middle Miocene, collision of the Bonin Arc into central Honshu resulted in back-arc closing and crustal shortening (Chough & Barg 1987). The tectonic reorganization resulting from the basin closing has created regional uplift and destruction of Miocene basins since late Miocene time (Ingle 1992; Yoon & Chough 1995). The north-northeast-trending Yangsan Fault commenced activity in the early–middle Miocene (Yoon & Chough 1995; Choi *et al.* 2002a), and the north-northwest-trending Ulsan Fault commenced activity in the late Miocene (Choi *et al.* 2002b), and therefore, these two faults may be associated with the tectonic events, respectively.

The Quaternary terrace deposits, which generally can be separated into five stages according to their topographic levels, were developed parallel to the coastline. The Eupchon Fault is developed in the third marine terrace from the bottom (approximately 34 m above sea level). A fault length of 400–500 m can be traced from lineaments on aerial photographs, by geophysical investigation, and from bore-hole data (Fig. 2). The age of the second and third marine terraces has been determined by the optically stimulated luminescence (OSL) or tephra methods. There are two broad groups of ages: 50–70 ka and 110–120 ka (Inoue *et al.* 2002; KOPEC 2002; Choi *et al.* 2003).

The marine terrace sediments are overall well sorted and bedded, but some parts are poorly sorted. Therefore, the sediments are interpreted as being a mixed sequence of marine and river terrace deposits, indicating a river channel environmental system around the coastline. Most of the sediments are composed of pebble-bearing sand and very coarse sand, generally showing fining-upward sequence (<20 cm pebble diameter). However, a lens-shaped mud layer (maximum thickness approximately 40 cm) is interbedded, and it is used as a key bed to measure the fault displacement because of its distinctive grain size compared to neighboring layers.

RESEARCH METHODS

A retaining wall now covers the original site of the fault; hence, it has been investigated in two new trench sites, located approximately 12 m to the

southwest of the original location. The orientations of the two trenches are 170° (Trench 1) and 150° (Trench 2) (Fig. 3), and they are oblique to the fault. The widths of Trench 1 and Trench 2 are 1.5 and 1.3 m, and the maximum depths are 5.5 and 2.8 m, respectively.

Maps of the two trench sections were made using 0.5×0.5 m grids, with some additional maps produced to provide details of specific structures. Based on the kinematic analyses, 3-D fault geometry and deformation history of this fault were reconstructed. An estimate of the fault length has been made based on an empiric relationship between displacement and length. The possibility of reactivation of the fault, based on the *in situ* stress conditions obtained by earthquake focal mechanism and tectonic analysis of fractures, is assessed.

TRENCH MAPPING

Two southwestern sections were constructed from the surface mapping of the trench sections by compiling photos (grid interval 0.5 m; Figs 4,5). These are approximately 8×4.5 m (Trench 1) and 5.5×2.5 m (Trench 2). Figure 4 shows a photo mosaic (Fig. 4a) and simplified sketch (Fig. 4b) of the southern side of Trench 1 (170°). The terrace sediments are relatively well sorted and well bedded, showing grain size variation of pebbles and matrix. A sedimentary sequence can be matched between the hanging wall and footwall blocks. Figures 4c and 4d show strata displaced into the footwall and hanging wall that are used to measure displacement across the fault. Manganese oxide layers, developed in the pebble-bearing sandstones, provide subsidiary evidence for displacement of the key beds.

Figure 5 shows the southern side section of Trench 2 (150°). The long axes of the pebbles show preferred orientation along the main fault plane (Figs 5c, 6a,c), which is a useful way of recognizing the fault plane in unconsolidated sediments. The fault system includes one main reverse fault (N20°E/40°SE) with 4.1 m displacement (approximately 2.5 m vertical separation) and a series of branch faults at the top of the Quaternary terrace sediments (Figs 4,5). The branch faults are mainly developed in the footwall, but small discrete faults are also developed at the hanging wall anticline (Fig. 4b,d). Imbrication (Dahlstrom 1970) or fault branching (Kim *et al.* 2003) at fault tips are very common damage patterns (Kim *et al.* 2004).

The main fault is termed Fault A (N03°E/38°SE) and the branch fault in the footwall is termed Fault B (N02°E/28°SE) (Figs 4,5). Fault A has a fault zone of approximately 5 cm in thickness, and Fault B is composed of an injected reddish gray fault gouge of approximately 1 cm in thickness. The fault gouge gets thinner downward along the fault plane, but thickens again at the junction with Fault A (N20°/40°SE), and then increases downward to approximately 10–20 cm in thickness. The dip of the joined fault is approximately 40°, similar to that of Fault A, and the displacement along Fault B is only approximately 60 cm. Therefore, Fault A is regarded to be the main fault and Fault B the branch fault at its tip (e.g. Kim *et al.* 2004). Pebbles along the main plane of Fault A show preferred orientation of their long axes indicating intense shearing deformation (Fig. 6c). The pebble layers also show drag folds (Figs 6a,b), indicating a movement direction of top-to-west (KIGAM 1998).

At the tip of Fault B, back thrusts, pop-up structures and branch faults are developed, indicating a fault tip damage zone (Kim *et al.* 2003, 2004). The displacement along the fault at the tip zone decreases from approximately 36 to 0 cm within 25 cm from the boundary between mud and unconsolidated pebble-bearing conglomerate layers. Therefore, the fault displacement may be abruptly terminated by this anisotrophic layer boundary (Peacock & Sanderson 1992).

Although the number of faulting events is another concern in the study of active faults, there is no clear evidence to interpret deformation events such as deformed colluvial wedges or stratigraphic offsets (e.g. Burbank & Anderson 2001; Keller & Pinter 2002). Therefore, further work is necessary to determine the number of deformation events along this fault.

THRUST GEOMETRIES

The Quaternary Eupchon Fault shows reverse-sense displacement with approximately 6 m vertical separation at the first exposed outcrop (KIGAM 1998). The strike and dip of the main fault is N15°E/45°SE, and the dip decreases upward. Slickenside lineations on the fault surface trend east–west, and the thickness of the fault gouge zone is approximately 20 cm (KIGAM 1998). Detailed thrust structures are excellently preserved in the unconsolidated sediments of this fault system. Hanging wall anticlines and drag of

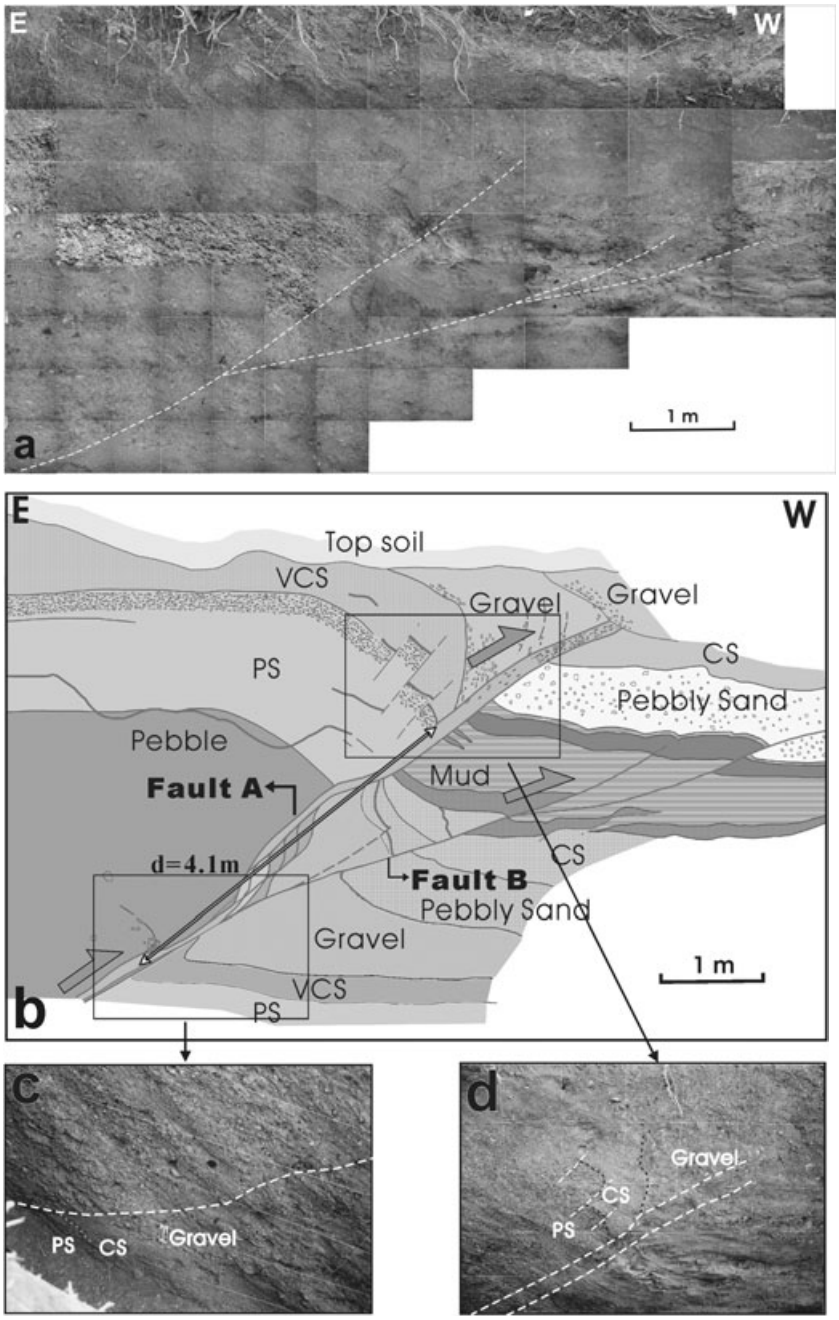

Fig. 4 Trench section on the south side of Trench 1. (a) Photo mosaic of the southern face of Trench 1. The fault traces are not clear, because they are mainly developed by preferred orientation of pebbles. (b) Simplified sketch map of the trench section showing several branch faults, drag folds and duplex geometries. (c,d) Detailed photographs of the strata sequences used to measure the displacement along the fault in footwall and hanging wall, respectively. CS, coarse sand; PS, pebble-bearing sand; VCS, very coarse sand.

interbedded pebble and sand layers are observed along the fault, indicating fault movement sense (Figs 4b, 6a,b). The drag folds indicate that thrusting occurred in a material exhibiting transitional brittle–ductile behavior, but without extensive loss of cohesion between grains. This probably means that the faulting in the unconsolidated sediments occurred under some confining pressure, in depth and/or with very rapid speed. During earthquakes, particles in the fault zone move relative to one another at velocities of the order of 0.1–1 m/sec, for durations of approximately 1–10 s (Cowan 1999).

The continuity of the branch fault is not clear at the top of the sediments (Fig. 6a), while the main fault plane is composed of a fault zone of approximately 10 cm in thickness, showing preferred orientation of pebbles (Fig. 6c). The main fault zone has a constant thickness and continues upward to the bottom of the wedge-shaped gravel layer (Figs 4,5). This may indicate that the fault was exposed to the surface until sedimentation of the

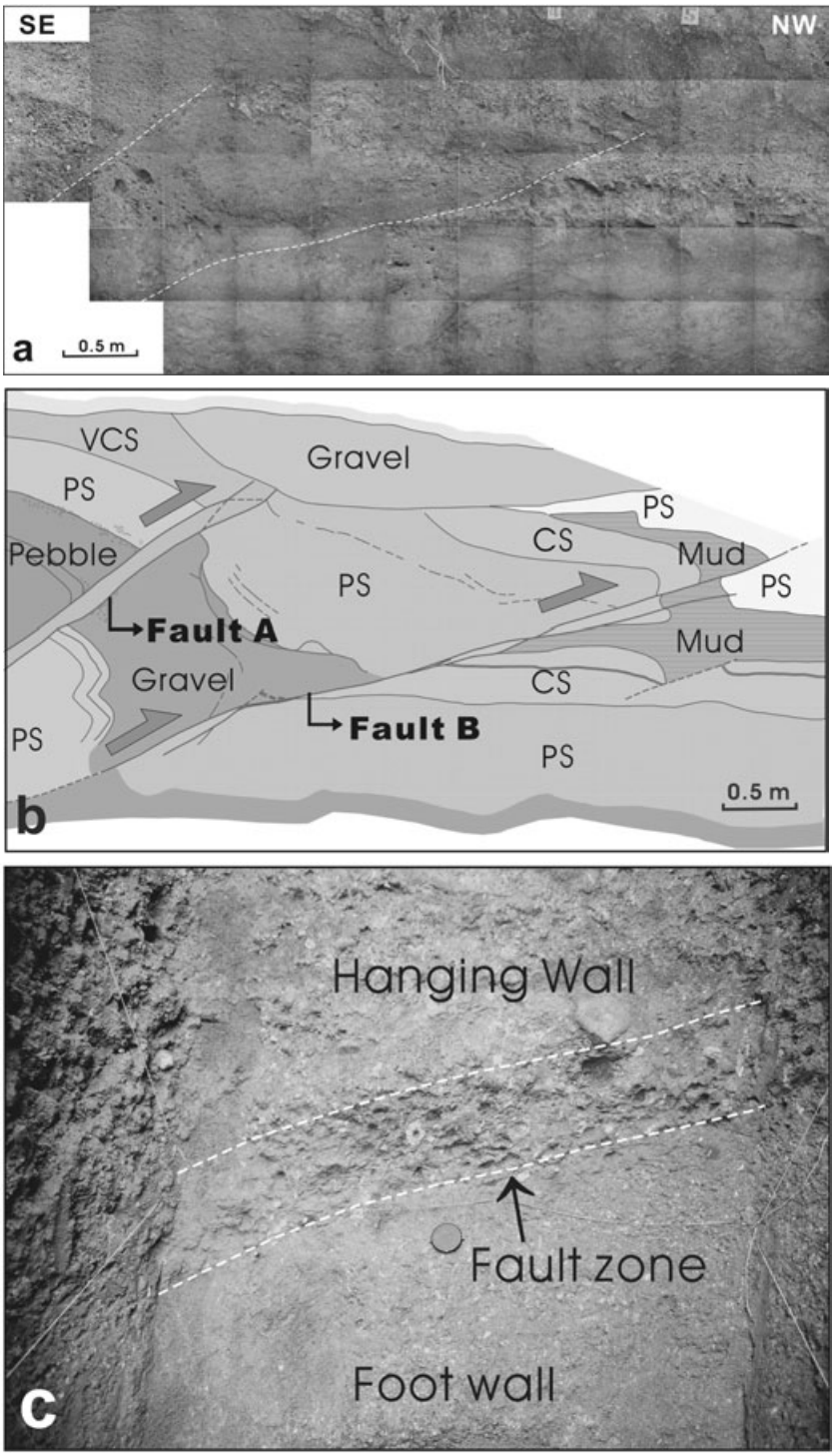

Fig. 5 Trench section on the south side of Trench 2. (a) Photo mosaic of the southern face of Trench 2. Fault traces are recognized by abrupt change of the grain sizes across the fault. (b) Simplified sketch map of the trench section showing several branch faults and drag folds. (c) The joined main fault zone at the bottom of Trench 2, looking to the southeast, showing strong preferred orientation of intermediate axes (*Y*-axis) of the pebbles compared to that outside the fault zone. CS, coarse sand; PS, pebble-bearing sand; VCS, very coarse sand.

overlying gravel layer. Therefore, the age of the gravel layer could limit the youngest age of the fault activity, although the age of the layer has not yet been determined.

Other thrust structures are back thrusts and pop-up structures (e.g. Butler 1982), or synthetic and antithetic faults on the northern side of Trench 1 (Fig. 6d). The light gray mud layer is popped up by compression. Also, well-developed small-scale thrust duplexes with flat-ramp geometries are observed on the south side of Trench 1 (Figs 4b, 6e,f). Coarse sand and pebble-bearing sand layers are repeated by thrusting, showing clear duplex geometries (Fig. 6e,f; e.g. Boyer & Elliott 1982;

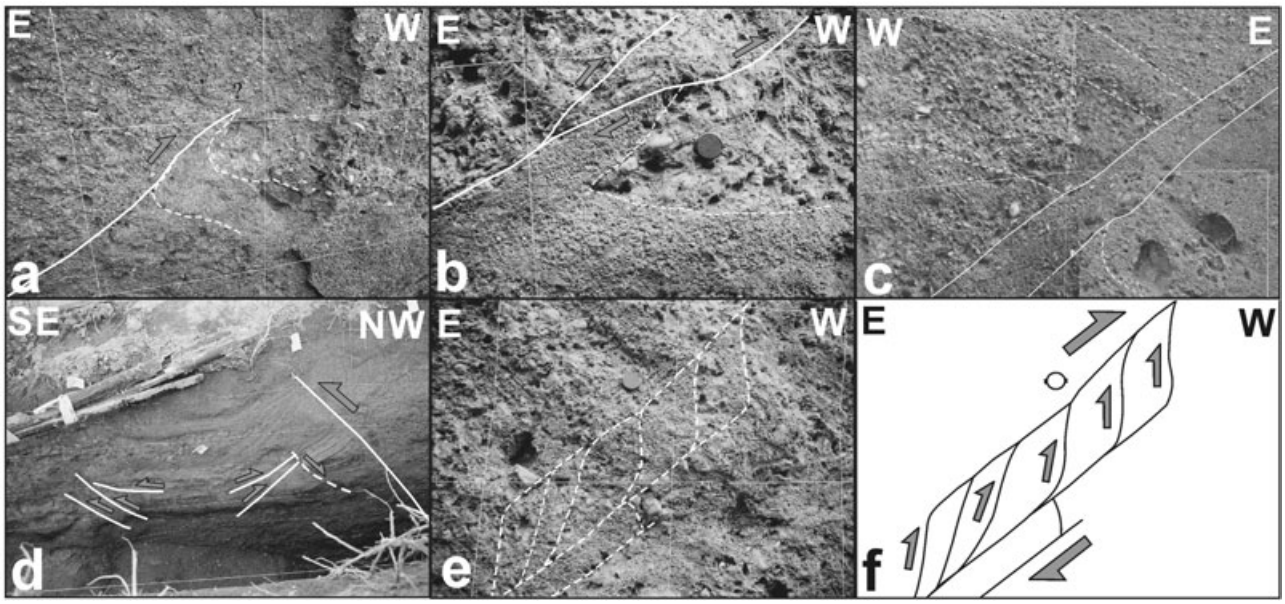

Fig. 6 Several thrust geometries observed on the trench surfaces. (a) Fault truncation and drag folds. (b) Branch faults and drag folds. (c) Fault zone showing preferred orientation of pebbles. (d) Pop-up structures and back thrusts cross-cutting mud layer. (e,f) Duplex geometries with several isolated lenses (horses) composed of different grain sizes. Camera lens cap (70 mm diameter) shows scale.

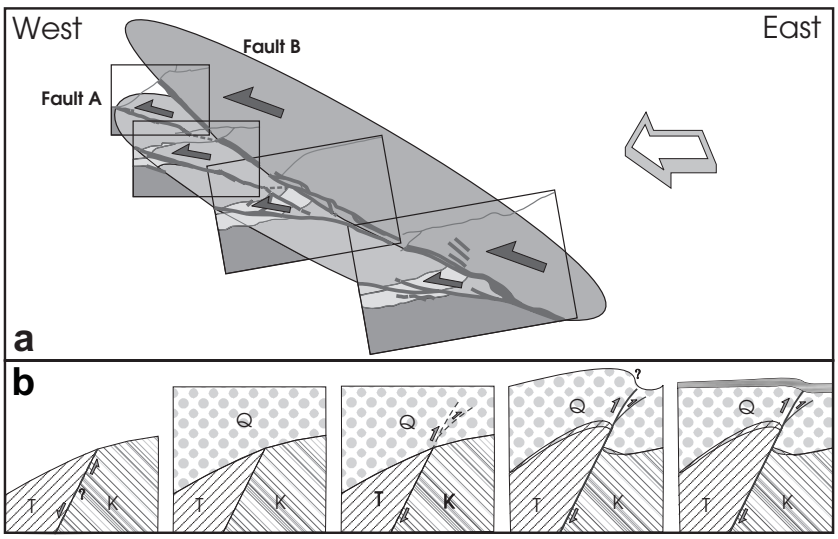

Fig. 7 3-D fault geometry and evolution model of the Eupchon Fault. (a) Reconstructed 3-D fault geometry based on combined fault maps from the trench sections. (b) Deformation history of the Eupchon Fault: early Tertiary normal faulting followed by Quaternary reverse faulting. The Quaternary Eupchon Fault most probably used the pre-existing normal fault for reactivation. K, Cretaceous sedimentary rocks; Q, Quaternary terrace sediments; T, Tertiary volcanic rocks.

Butler 1982; Bowler 1987). The extensive development and variety of these thrust structures in unconsolidated sediments is unusual, and suggests some ductility of the material without loss of cohesion. This may have enhanced the development of the duplex geometry in response to the relatively short displacement on the fault.

DEFORMATION MODELS

To understand the 3-D fault geometry of the Eupchon Fault, we illustrate a 3-D sliced block diagram from the four section data of the two trench surveys (Fig. 7a). The fault has a series of branches in the footwall taking off from the main fault. The displacement of the fault decreases toward the southwest, indicating a fault center to the northeast. This agrees with the displacement of approximately 6 m vertical separation observed at the original outcrop approximately 12 m to the northeast (KIGAM 1998). Therefore, the maximum displacement along the fault is at least 8.5 m (≈6 m/sin45°).

Before deposition of the Quaternary sediments, the Eupchon Fault was a normal fault, down

throwing Tertiary andesites against the Cretaceous sedimentary rocks. This relationship was reported from the rock sequence at the first outcrop found (KIGAM 1998). The unconformity surface between the Quaternary deposits and the underlying basements was displaced later in a reverse sense by at least 8.5 m.

Figure 7b shows an evolutionary model of the Eupchon Fault. In Stage 1, the Tertiary andesitic rocks made contact with Cretaceous sedimentary rocks by normal faulting, dipping to the east. This extensional stage may be associated with the opening of the East Sea in late Oligocene to early Miocene time (e.g. Kimura & Tamaki 1986; Tamaki 1988; Kaneoka *et al.* 1992; Yoon & Chough 1995). In Stage 2, Quaternary terrace sediments were deposited on the erosional surface, and in Stage 3, thrust faulting, drag of sediment layers and branch faulting developed by east–west compression during the Quaternary. This compressional stage may be associated with the closing of the East Sea since late Miocene time (e.g. Ingle 1992; Yoon & Chough 1995). In Stage 4, the fault scarp and hanging wall anticline was eroded, and in Stage 5, the top gravels were deposited on the erosional surface (colluvial wedge; e.g. Burbank & Anderson 2001; Keller & Pinter 2002). There is no evidence for the deformation of the gravels.

DISCUSSION

Because of poor exposure and discontinuity of the terrace sediments, estimation of fault length can only be inferred from limited observations and from aerial photo lineaments, geophysical surveys and bore-hole data. Another approach is to use empirical relationships between displacement and fault length (e.g. Peacock & Sanderson 1996; Park *et al.* 2003). The inferred fault length from direct observation and from measurement of the displacement of the Quaternary fault (~8.5 m) is 200–2000 m, without consideration of normal faulting and reactivation effect (Fig. 8; Park *et al.* 2003). However, the use of maximum displacement–fault length relationship from consolidated rocks is very questionable, because the fault is developed in unconsolidated sediments. Therefore, further studies and data are necessary to infer the lengths of faults developed in unconsolidated sediments.

The regional stress orientation estimated from analysis of the Eupchon Fault is similar to the current stress state from several other studies (e.g. June 1991; Choi *et al.* 2002b). The current stress state inferred from earthquake focal mechanism and tectonic analysis of fractures is slightly rotated anticlockwise from east–west (Fig. 9; Choi *et al.* 2002a). The orientation of the maximum compressive stress is generally east-northeast–west-southwest, and the attitude of the Eupchon Fault is N15–20°E/40–45°SE. Therefore, the fault should be reactivated as an oblique slip fault with reverse and right-lateral components, if sufficient stress accumulates (Fig. 10).

For earthquake hazard analysis, the age and recurrence interval of a fault are very important. The OSL ages of the lower gravel and pebble-bearing sandstone layers from the trench site were reported to be 67 ± 5 ka and 63 ± 12 ka, respectively (KOPEC 2002). However, the tephra correlation age from the younger second terrace by refractive index correlation was reported to be 100–110 ka (Inoue *et al.* 2002). The OSL ages from the second and the third terraces form two broad groups at 50–70 and 110–120 ka (Choi *et al.* 2003), and Choi *et al.* (2003) interpret the broad age groups to be the result of tectonic activity during the Late Pleistocene. Therefore, the ages of the marine terrace and the fault activity are not fixed yet, and further studies are in progress to determine them.

CONCLUSIONS

The Eupchon Fault cross-cuts Quaternary marine terraces in southeast Korea. A variety of Quaternary thrust fault structures (i.e. preferred orientation of pebbles, branch fault, drag fold, pop-up, back thrust and duplex) are well preserved in the unconsolidated sediments.

1. The deformation patterns of the Eupchon Fault in unconsolidated Quaternary sediments are very similar to thrust geometries in consolidated rocks. The well-preserved thrust geometries may result from rapid thrust movement of partially consolidated sediments showing brittle–ductile properties.
2. The Eupchon Fault has experienced inversion. Early Tertiary faulting was normal, related to extension of the East Sea. The fault was reactivated as a reverse or thrust fault during the Quaternary.
3. The inferred minimum fault length developed

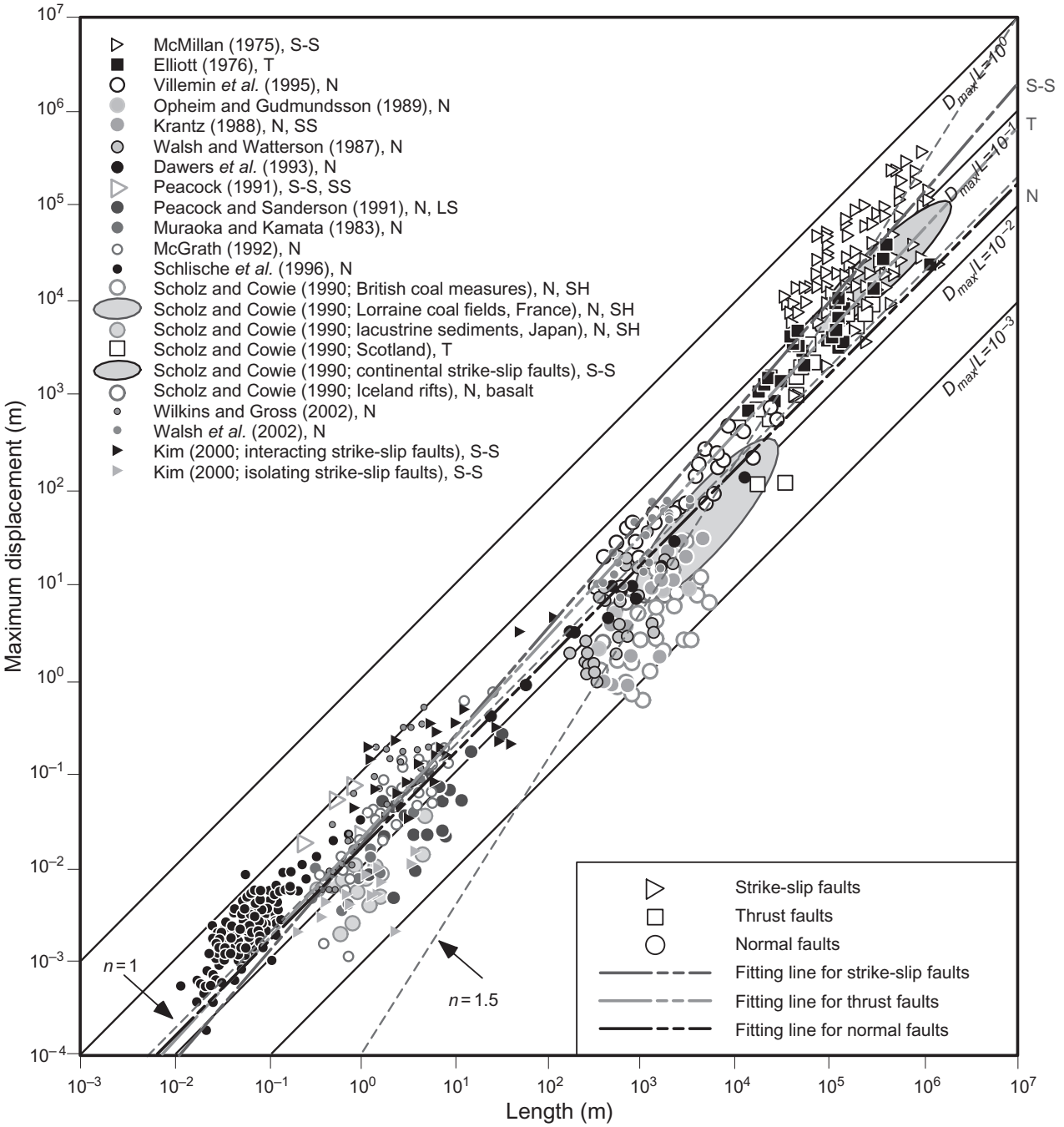

Fig. 8 Inferred fault length of the Quaternary Eupchon Fault. The estimated fault length from the empiric relationship between maximum displacement and fault length is approximately 200– 2000 m, without considering reactivation. The graph is combined from data in several previously published reports: McMillan (1975); Elliott (1976); Muraoka and Kamata (1983); Walsh and Watterson (1987); Krantz (1988); Opheim and Gudmundsson (1989); Scholz and Cowie (1990); Peacock (1991); Peacock and Sanderson (1991); Dawers *et al.* (1993); Villemin *et al.* (1995); Schlische *et al.* (1996); Kim (2000); Walsh *et al.* (2002); Wilkins and Gross (2002). LS, limestones; N, normal faults; SH, shales; SS, sandstones; S-S, strike-slip faults; T, thrust faults.

during Quaternary thrust faulting, determined from displacement and other direct investigations, is 400–2000 m.

4. The regional stress condition inferred from the fault analysis is similar to the current stress regime determined from several studies, with slight rotation. This suggests that if the fault is reactivated, some oblique slip with reverse and right-lateral components may be involved in the reactivation.

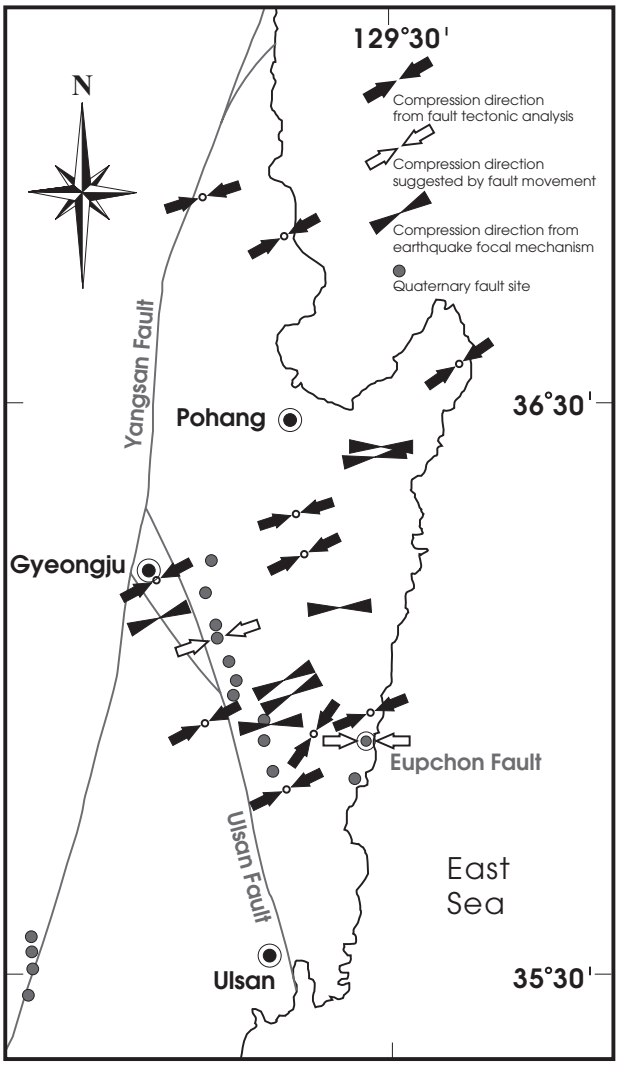

Fig. 9 Regional stress conditions around the Eupchon Fault inferred from earthquake data, paleostress analysis and fault plane analysis (modified from June 1991; Choi *et al.* 2002b). The current general maximum compressive stress axis is almost an east-northeast–west-southwest trend.

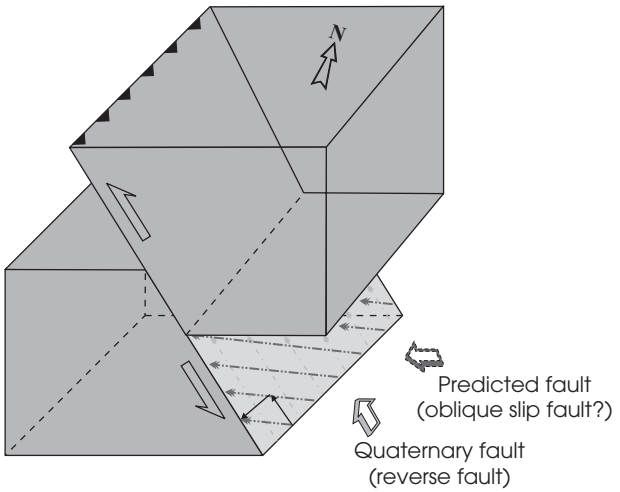

Fig. 10 Schematic diagram of the possible reactivation of the Quaternary Eupchon Fault. The fault has clearly observed features indicating reverse slip, but from its orientation relative to the present-day stress field, might be expected to be oblique slip, with reverse and right-lateral slip components.

ACKNOWLEDGEMENTS

We thank J. H. Hwang, Y. J. Kim and J. B. Kyung for constructive discussions. We also thank C. D. Park for his fieldwork. The paper was improved by reviews from Yujiro Ogawa and Yuji Kanaori. This work was funded by KOPEC and MOCIE of Korean government (R-2002-0-279).

REFERENCES

BOWLER S. 1987. Duplex geometry: an example from the Moine Thrust Belt. *Tectonophysics* **135**, 25–35.

BOYER S. E. & ELLIOTT D. 1982. Thrust systems. *American Association of Petroleum Geologists Bulletin* **66**, 1196–230.

BURBANK D. W. & ANDERSON R. S. 2001. *Tectonic Geomorphology*. Blackwell Science, Abingdon.

BUTLER R. W. H. 1982. The terminology of structures in thrust belts. *Journal of Structural Geology* **4**, 239–45.

CHANG T. W. 2001. Quaternary tectonic activity at the eastern block of the Ulsan fault. *Journal of the Geological Society of Korea* **37**, 431–44 (in Korean with English abstract).

CHOI J. H., MURRAY A. S., JAIN M., CHEONG C. S. & CHANG H. W. 2003. Luminescence dating of well-sorted marine terrace sediments on the southeastern coast of Korea. *Quaternary Science Reviews* **22**, 407–21.

CHOI P.-Y., KWON S.-K., LEE S. R., HEANG J.-H., ANGELIER J. & AN G.-O. 2002a. Late Mesozoic-Cenozoic tectonic sequence of Southeast Korea. *In* Jin M. S. (ed.) *Mesozoic Sedimentation, Igneous Activity and Mineralization in South Korea*, The 1st and 2nd Symposiums on the Geology of Korea, Special Publication no. 1, pp. 52–88. Korea Institute of Geoscience and Mineral Resources, Daejeon.

CHOI P.-Y., RYOO C.-R., KWON S.-K. *et al.* 2002b. Fault tectonic analysis of the Pohang-Ulsan area, SE Korea: Implications for active tectonics. *Journal of the Geological Society of Korea* **38**, 33–50.

CHOUGH S. K. & BARG E. 1987. Tectonic history of Ulleung basin margin, East Sea (Sea of Japan). *Geology* **15**, 45–8.

COWAN D. S. 1999. Do faults preserve a record of seismic slip? A field geologist's opinion. *Journal of Structural Geology* **21**, 995–1001.

DAHLSTROM C. D. A. 1970. Structural geology in the eastern margin of the Canadian rocky mountains. *Bulletin of Canadian Petroleum Geology* **18**, 332–406.

DAWERS N. H., ANDERS M. H. & SCHOLZ C. H. 1993. Growth of normal faults: Displacement-length scaling. *Geology* **21**, 1107–110.

ELLIOTT D. 1976. Energy balance and deformation mechanisms of thrust sheets. *Royal Society of London Philosophical Transactions, Series A* **283**, 289–312.

INGLE J. C. Jr 1992. Subsidence of the Japan Sea: Stratigraphic evidence from ODP Sites and onshore sections. *Proceedings, Ocean Drilling Program, Scientific Results* **127/128**, 1197–281.

INOUE D., SASAKI T., YANAGIDA M., CHOI W. H. & CHANG C. J. 2002. Stratigraphy of the marine terraces along the east coast in Korea by means of the loess-paleosol sequence and Japanese tephra. *The 55th Geological Society of Korea Conference Abstract Volume*, p. 81. Kongju National University.

JUN M.-S. 1991. Body-wave analysis for shallow intraplate earthquakes in the Korean Peninsula and Yellow Sea. *Tectonophysics* **192**, 345–57.

KANEOKA I., TAKIGAMI Y., TAKAOKA N., YAMASHITA S. & TAMAKI K. 1992. ^{40}Ar-^{39}Ar analysis of volcanic rocks recovered from the Japan Sea floor: Constraints on the age of formation of the Japan Sea. *Proceedings, Ocean Drilling Program, Scientific Results* **127/128**, 819–36.

KELLER E. A. & PINTER N. 2002. *Active Tectonics: Earthquakes, Uplift, and Landscape*, 2nd edn. Prentice Hall, New Jersey.

KIM Y.-S. 2000. Damage structures and fault evolution around strike-slip faults. PhD Thesis. University of Southampton, Southampton.

KIM Y.-S., PEACOCK D. C. P. & SANDERSON D. J. 2003. Mesoscale strike-slip faults and damage zones at Marsalforn, Gozo Island, Malta. *Journal of Structural Geology* **25**, 793–812.

KIM Y.-S., PEACOCK D. C. P. & SANDERSON D. J. 2004. Fault damage zones. *Journal of Structural Geology* **26**, 503–517.

KIMURA G. & TAMAKI K. 1986. Collision, rotation, and back-arc spreading in the region of the Okhotsk and Japan Seas. *Tectonics* **5**, 389–401.

KOREA INSTITUTE OF GEOLOGY, MINING AND MATERIALS (KIGAM). 1998. *An Investigation and Evaluation of Capable Fault: Southeastern Part of the Korean Peninsula.* KIGAM, Daejeon (in Korean with English abstract).

KOREA POWER ENGINEERING COMPANY (KOPEC). 2002. *The Preliminary Site Assessment Report (PSAR) for the New Weolsung Reactors 1 and 2*, Unpulished Report. KOPEC, Yongin.

KRANTZ R. W. 1988. Multiple fault sets and three-dimensional strain. *Journal of Structural Geology* **10**, 225–37.

KYUNG J. B. & CHANG T. W. 2001. The latest fault movement on the northern Yangsan fault zone around the Yugye-ri area, southeast Korea. *Journal of the Geological Society of Korea* **37**, 563–77 (in Korean with English abstract).

LEE J. I. 2000. Provenance and thermal maturity of the lower Cretaceous Gyeongsang Supergroup, Korea. PhD Thesis. Seoul National University, Seoul.

MCMILLAN R. A. 1975. The orientation and sense of displacement of strike-slip faults in continental crust. Bachelor's Thesis. Carleton University, Ottawa, Ontario.

MURAOKA H. & KAMATA H. 1983. Displacement distribution along minor fault traces. *Journal of Structural Geology* **5**, 483–95.

OPHEIM J. A. & GUDMUNDSSON A. 1989. Formation and geometry of fractures, and related volcanism, of the Krafla fissure swarm, northeast Iceland. *Geological Society of America Bulletin* **101**, 1608–22.

PARK J. Y., KIM Y.-S., KIM J. H. & SHIN H. C. 2003. Thrust geometries in unconsolidated Quaternary sediments around the Eupchon fault, SE Korea. *In EGS-AGU-EUG Joint Assembly*, Abstract Volume, pp. EAE03–A-02069; SM13–1M02P-0261. Nice, France.

PEACOCK D. C. P. 1991. Displacement and segment linkage in strike-slip fault zones. *Journal of Structural Geology* **13**, 1025–35.

PEACOCK D. C. P. & SANDERSON D. J. 1991. Displacement and segment linkage and relay ramps in normal fault zones. *Journal of Structural Geology* **13**, 721–33.

PEACOCK D. C. P. & SANDERSON D. J. 1992. Effects of layering and anisotropy on fault geometry. *Journal of Geological Society of London* **149**, 793–802.

PEACOCK D. C. P. & SANDERSON D. J. 1996. Effects of propagation rate on displacement variations along faults. *Journal of Structural Geology* **18**, 311–20.

REE J.-H., LEE Y.-J., RHODES E. J. *et al.* 2003. Quaternary reactivation of Tertiary faults in the southeastern Korean Peninsula: Age constraint by optically stimulated luminescence dating. *The Island Arc* **12**, 1–12.

RYOO C.-R., LEE B. J. & CHWAE U. 2000. Quaternary fault and its remote sensing image in the southeastern Korea. *CCOP Technical Bulletin* **29**, 5–28.

RYOO C.-R., LEE B. J., SON M., LEE Y. H., CHOI S.-J. & CHWAE U. 2002. Quaternary faults in Gaegok-ri, Oedong-eup, Gyeongju, Korea. *Journal of the Geological Society of Korea* **38**, 309–23.

SCHLISCHE R. W., YOUNG S. S., ACKERMANN R. V. & GUPTA A. 1996. Geometry and scaling relations of a population of very small rift-related normal faults. *Geology* **24**, 683–6.

SCHOLZ C. H. & COWIE P. A. 1990. Determination of geologic strain from fault slip data. *Nature* **346**, 837–9.

TAMAKI K. 1988. Geological structure of the Japan Sea and its tectonic implications. *Bulletin of the Geological Survey of Japan* **39**, 269–365.

VILLEMIN T., ANGELIER J. & SUNWOO C. 1995. Fractal distribution of fault length and offsets: Implications of brittle deformation evaluation—Lorraine Coal Basin. *In* Barton C. C. & La Pointe P. R. (eds.) *Fractal in the Earth Sciences*, pp. 205–26. Plenum Press, New York.

WALSH J. J., NICOL A. & CHILDS C. 2002. An alternative model for the growth of faults. *Journal of Structural Geology* **24**, 1669–75.

WALSH J. J. & WATTERSON J. 1987. Distributions of cumulative displacement and seismic slip on a single normal fault surface. *Journal of Structural Geology* **9**, 1039–46.

WILKINS S. J. & GROSS M. R. 2002. Normal fault growth in layered rocks at Split Mountain, Utah: influence of mechanical stratigraphy on dip linkage, fault restriction and fault scaling. *Journal of Structural Geology* **24**, 1413–29.

YOON S. H. & CHOUGH S. K. 1995. Regional strike-slip in the eastern continental margin of Korea and its tectonic implications for the evolution of Ulleung Basin, East Sea (Sea of Japan). *Geological Society of America Bulletin* **107**, 83–97.